Experimental performance of a fully tunable complex-coefficient optical FIR filter using wavelength conversion and chromatic dispersion

Salman Khaleghi,[1,*] Mohammad Reza Chitgarha,[1] Omer F. Yilmaz,[1] Moshe Tur,[2] Michael W. Haney,[3] Carsten Langrock,[4] Martin M. Fejer,[4] and Alan E. Willner[1]

[1]*Department of Electrical Engineering, University of Southern California, Los Angeles, California 90089, USA*

[2]*School of Electrical Engineering, Tel Aviv University, Ramat Aviv 69978, Israel*

[3]*Department of Electrical and Computer Engineering, University of Delaware, Newark, Delaware 19716, USA*

[4]*Edward L. Ginzton Laboratory, Stanford University, Stanford, California 94305, USA*

**Corresponding author: khaleghi@usc.edu*

Received April 4, 2012; revised June 12, 2012; accepted July 2, 2012;
posted July 3, 2012 (Doc. ID 166071); published August 9, 2012

We experimentally characterize the performance of a continuously tunable all-optical complex-coefficient finite-impulse-response (FIR) filter that exploits nonlinear signal processing (multiplexing and multicasting) and conversion-dispersion-based optical delays. Various length (three and four) optical FIR filters with different tap amplitudes (from 0 to –9 dB), tap phases (from 0 to 2π), and tap delays (~37.4 ps and 25 ps) are realized, showing reconfiguration and tuning capabilities of this FIR filter. The measured frequency responses show close agreement with the theoretical filter responses.

OCIS codes: 060.2360, 060.4370, 190.4223.

A key building block for many signal processing functions is a finite-impulse-response (FIR) filter, that can be used for matched filtering, equalization, pulse shaping, and correlation [1–3]. Implementation of FIR filters requires time-delayed taps, with each tap weighted by a variable complex (amplitude and phase) coefficient. For many years, there has been a keen interest in the possibility of realizing FIR filters all-optically in order to utilize the high bandwidth of optics and achieve transparent operation. Given that tunable filters are more useful than the fixed filters, a crucial goal would be the continuous tunability of the optical FIR filters' characterization [4].

Utilization of the large bandwidth of photonic technologies for high-speed signal processing may require implementation of FIR filters all-optically. An optical method can potentially advance significantly the performance of signal processing when the signal to be processed is at high speed or is a combination of many lower-speed signals [5]. Recent works that involve optical FIR filters have been based on technologies such as fixed fiber-based delays [6], integrated cascaded Mach–Zehnder interferometers [5], integrated ring-resonator-based filters [7–9], beating between frequency combs [4], and microwave photonics techniques [2]. Most of these approaches are generally fixed or are tunable over finite or discrete ranges, and tend not to have independent control over the amplitude, phase, and delay of each tap of the FIR filter. Therefore, a laudable goal would be to demonstrate an FIR filter in which all critical parameters of the FIR filter (i.e., the FIR length, amplitudes, phases and delays) are tunable.

In this Letter, we experimentally characterize the performance of a tunable optical FIR filter with complex coefficients that achieves reconfigurability through the use of nonlinearity-based wavelength conversions and chromatic-dispersion-based delays [10,11]. In our scheme, the second-order susceptibility ($\chi^{(2)}$) in the periodically poled lithium niobate (PPLN) waveguides is exploited to realize signal multicasting and multiplexing. Tunable optical delays are realized using the frequency-depend speed of light in a dispersion compensating fiber (DCF) [11]. Phase coherent multiplexing is made possible by reusing the same pump lasers that are initially used for wavelength multicasting. We experimentally assessed the tuning of tap amplitudes from 0 dB to –9 dB, tap phases (0 to 2π), and the delays (~37.4 ps and ~25 ps) by measuring the filters' frequency responses. The measurements show close agreement with theoretical filter responses.

For a length-N FIR filter with N taps taken at times T_i and weighted by complex-coefficients h_i, the relation between the input signal $x(t)$ and the output signal $y(t)$ is determined by $y(t) = \sum_{i=1}^{N} h_i x(t - T_i)$. Therefore, the FIR filter can be tuned and reconfigured by changing the number of taps (N), tap delays (T_i), and complex tap coefficients (h_i). Figure 1 shows the conceptual

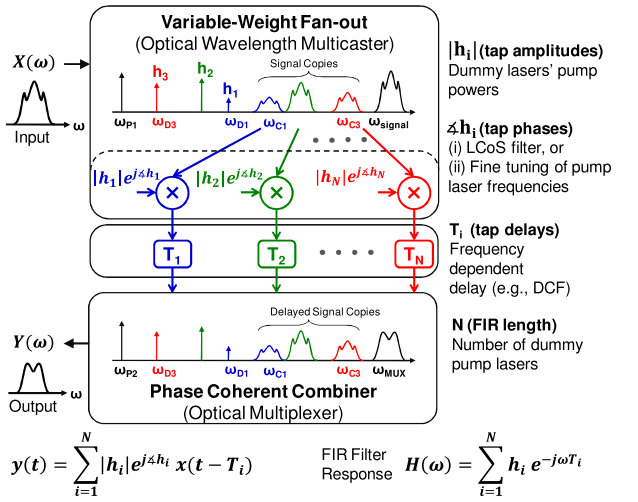

Fig. 1. (Color online) Conceptual block diagram of the tunable complex-coefficient optical FIR filter.

block diagram of the tunable complex-coefficient FIR filter. First, a nonlinear optical mixer and multiple tunable dummy pump lasers fan-out N ($N = 3$ in Fig. 1) copies of the input data signal, with each signal copy located at a different center frequency. Subsequently, these replicas travel through a dispersive medium (e.g., DCF) at different speeds resulting in a different time delay on each signal copy. Finally, these copies are multiplexed together in a phase-preserving scheme by another high-speed nonlinear mixer, creating an output signal that is filtered by the FIR filter. Each signal copy generated in the fan-out stage represents a tap in the FIR filter and thus the taps can be accurately tuned in terms of amplitude, phase and relative time delay. PPLN waveguides are used as the nonlinear optical wave-mixer. These mixing interactions are governed by conservation of energy and phase-matching conditions [12]. In the fan-out stage, cascaded $\chi^{(2)}$ processes of sum frequency generation (SFG) and difference frequency generation (DFG) create copies of an amplitude/phase encoded input signal (ω_{signal}) [12]. In the first nonlinear stage the signal at ω_{signal} mixes with a continuous-wave (CW) pump laser at frequency ω_{P1}. The signal and the dummy pump frequencies are located at equal distance from the quasi-phase-matching frequency (ω_{QPM}). According to the "conservation of energy rule," this generates a sum frequency term at $\omega_{\text{signal}} + \omega_{P1}$, which is followed by multiple (N) DFG processes with the aid of N other CW dummy pump lasers at ω_{Di}. Consequently, copies of the signal will be generated at frequencies $\omega_{Ci} = \omega_{\text{signal}} + \omega_{P1} - \omega_{Di}$. After passing through the DCF, each signal copy (tap) is delayed by $T_i = \beta_2\ L(\omega_{Ci} - \omega_{C1}) = \beta_2\ L(\omega_{D1} - \omega_{Di})$ relative to the first tap (β_2 is the group velocity dispersion parameter). Similarly, cascaded SFG-DFG processes are used in another PPLN waveguide with the same QPM frequency as the first PPLN waveguide for optical multiplexing. To maintain the relative phase of taps in the multiplexing stage, the dummy pumps from the fan-out stage are filtered together with the signal copies (taps) in a phase/amplitude programmable filter based on liquid crystal on silicon (LCoS) technology. The LCoS filter, passes the signal copies and the dummy pumps and blocks the signal and ω_{P1} pump. Additionally, it applies the tap phases (φ_i) on the dummy pumps (ω_{Di}). Therefore, the dummy pumps are reused for the SFG mixings followed by DFG mixing using another CW pump laser at ω_{P2}. Thus, all taps are multiplexed to the frequency $\omega_{\text{MUX}} = \omega_{Ci} + \omega_{Di} - \omega_{P2} = \omega_{\text{signal}} + (\omega_{P1} - \omega_{P2})$ to create the FIR filter output. If same pump lasers ($\omega_{P1} = \omega_{P2}$) are used in both nonlinear stages, the FIR filter output is generated at the same center frequency as the input signal. Governed by the "phase matching conditions" in nonlinear wave mixings, each tap contributes to the multiplexed output proportional to

$$e^{j\phi_i} E^*_{P2} E_{Di} E^*_{Di} E_{P1} E_{\text{signal}}(t - T_i), \tag{1}$$

in which E denotes the electrical field amplitude and E^* is its complex conjugate. Neglecting the common terms between the taps (that do not depend on the index i), the resulting output signal of the FIR filter is proportional to

$$E_{\text{MUX}}(t) \propto \sum_{i=1}^{N} e^{j\phi_i} |E_{Di}|^2 E_{\text{signal}}(t - T_i). \tag{2}$$

Therefore, the FIR length (N, number of taps) can be varied by adding/removing dummy pump lasers, FIR delays T_i can be continuously varied by tuning the dummy pumps' frequencies, and FIR tap amplitudes are directly controlled by the dummy pumps' powers. The FIR filter tap phases can be applied using the LCoS filter or by adding a fine offset to the dummy pump wavelengths.

Figure 2 depicts the experimental setup. A vector network analyzer (VNA) sweeps the frequencies from ~0 to 40 GHz to modulate a ~1538.5 nm laser (ω_{signal}) using a Mach–Zehnder modulator biased at the quadrature point. This input signal, a ~1562.5 nm CW pump laser (ω_{P1}), and four CW dummy pump lasers (ω_{D1} to ω_{D4}) are separately amplified, filtered, coupled together and sent into a 4 cm PPLN waveguide. The cascaded SFG-DFG processes in the first PPLN waveguide create copies of the signal (ω_{C1} to ω_{C4}). The LCoS-based filter after the PPLN waveguide passes the dummy pumps (ω_{Di}) and the signal copies (ω_{Ci}) and cuts off the signal and the ω_{P1} pump. The LCoS filter also applies the variable tap phases on the dummy pumps, as shown in Fig. 2b. The signal copies and the dummy pumps are sent to an $L \approx 195$ m DCF to induce the relative delays between copies. The DCF has chromatic dispersion of $D \approx -80$ ps /nm /km, resulting in $D \times L = 15.6$ ps /nm dispersion for the DCF spool. The signal copies and the pump lasers are then amplified and sent to a 5 cm PPLN waveguide, along with another CW pump laser (ω_{P2}) at ~1562.5 nm. The QPM wavelength of both the first and the second PPLN waveguides are temperature tuned to ~1550.5 nm. Therefore, the wave mixings in the second PPLN waveguide can produce mixing products in a reciprocal fashion and generate a multiplexed output signal at the center frequency of the original input signal. Since $\omega_{P2} = \omega_{P1}$ the FIR filter's output is formed at ω_{signal} and is filtered out, amplified, sent to a photodetector and fed back to the VNA. The VNA characterizes the amplitude and phase response of the optical FIR filter.

Table 1 shows the reconfiguration capability of the FIR filter for various symbol rates. In order to configure the FIR filter for input signals with 40 Gbaud symbol rate, the tap delays of the filter need to be separated by

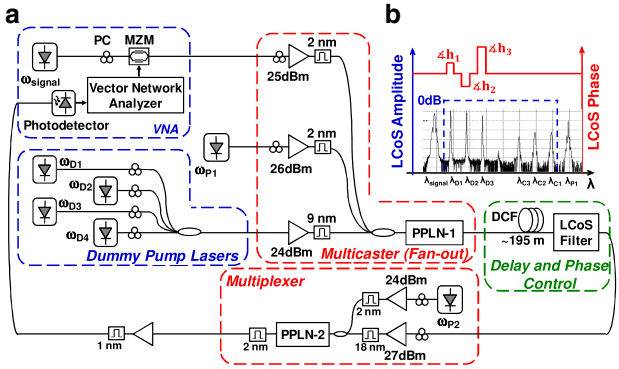

Fig. 2. (Color online) (a) Experimental setup: multicaster, delay, phase control, and multiplexer; (b) generic LCoS filter amplitude/phase profile for applying phases on the pumps.

Table 1. Optical FIR Capability to Accommodate Different Baud Rates Using Tunable Delays; $D \times L = 15.6$ ps/nm

Wavelength Separation, $\Delta\lambda$	Symbol Time, $\Delta T = (D \times L) \times \Delta\lambda$	Digital Filter Symbol Rate, $1/\Delta T$	Analog Filter FSR, FSR $= 1/\Delta T$
1.6 nm	25 ps	40 Gbaud	40 GHz
2.4 nm	37.4 ps	26.7 Gbaud	26.7 GHz

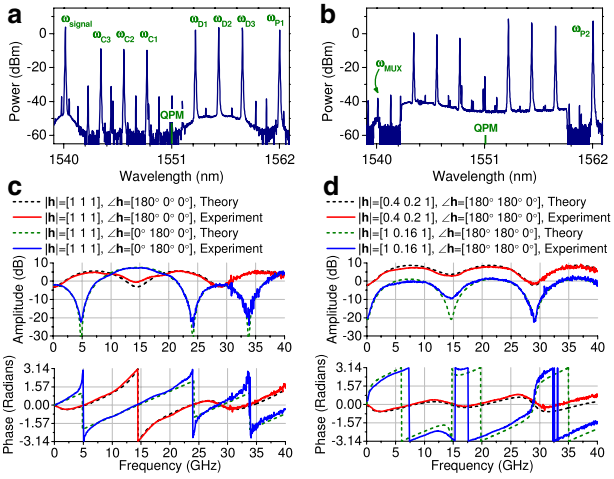

Fig. 3. (Color online) Wave mixing spectra for (a) fan-out stage, and (b) multiplexing stage. (c),(d) Experimental and theoretical amplitude/phase response of ~26.7 GHz FSR length-3 FIR filters.

25 ps. Therefore, the wavelengths of adjacent dummy pumps should be 1.6 nm apart, so that after passing through 15.6 ps/nm dispersion the taps experience 25 ps relative delay. If the adjacent tap delays are equal (i.e., $T_i = (i-1)\Delta T$) the resulting filter will be periodic with a free spectral range (FSR) of $1/\Delta T$. To tune to a different input signal rate (or filter FSR), the wavelength separation is increased to 2.4 nm resulting in filters with 26.7 GHz FSR.

Figure 3a depicts the measured spectrum after the multicasting stage for a length-3 FIR filter with ~37.4 ps delay (i.e., 2.4 nm wavelength spacing). In Fig. 3b, the output spectrum of the multiplexing stage is shown and the tap phases are set to create a null at the center frequency (destructive interference, 120° phase differences). The frequency responses of the FIR filters are measured and shown together with normalized theoretical responses in Fig. 3c and 3d. The measurements are normalized with respect to one-tap operation. To demonstrate tap-coefficient tuning, in Fig. 3c, all taps are set to have equal amplitudes and their phases are tuned using the LCoS filter. In Fig. 3d, amplitudes are varied by tuning laser powers in the first stage and the phases are kept the same (3 dB attenuation results in a 0.5 factor in "$|h|$"). Length-4 FIR filters with FSR ~40 GHz are realized in Fig. 4, where pump separations are set to 1.6 nm to induce ~25 ps delay between the taps. Similarly, the tuning capabilities of the length-4 FIR filters are demonstrated in Fig. 4c and 4d. Dummy laser powers are varied from 0 to −9 dB resulting in tap-amplitudes of 1 to 0.125. The differences between the theoretical responses and the measurements could be

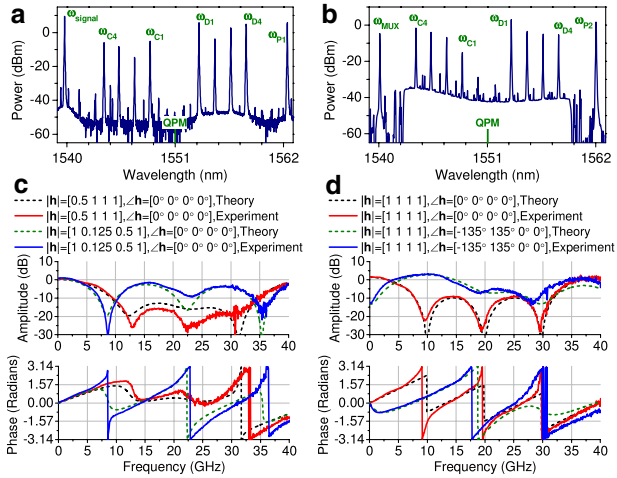

Fig. 4. (Color online) Wave mixing spectra for (a) fan-out stage, and (b) multiplexing stage. (c),(d) Experimental and theoretical amplitude/phase response of 40 GHz FSR length-4 FIR filters.

the result of limitation of the LCoS-filter resolution (~5°) and/or polarization variations effects. The VNA frequency response measurements show close agreement with the theory. The VNA bandwidth is limited to 40 GHz, but the FSR of the filter can potentially be made wider than 40 GHz by choosing smaller delays. The reconfiguration time of the filter is determined by the update speeds of the LCoS technology and pump wavelength tuning.

We acknowledge the support of Defense Advanced Research Projects Agency (DARPA) under the contracts FA8650-08-1-7820, N00014-05-1-0053 and W911NF-10-1-0151.

References

1. J. G. Proakis, *Digital Communications* (McGraw-Hill, 2000).
2. J. Yao, J. Lightwave Technol. **27**, 314 (2009).
3. T. Mengual, B. Vidal, and J. Martí, Opt. Commun. **281**, 2746 (2008).
4. V. R. Supradeepa, C. M. Long, R. Wu, F. Ferdous, E. Hamidi, D. E. Leaird, and A. M. Weiner, Nat. Photon. **6**, 186 (2012).
5. C. R. Doerr, S. Chandrasekhar, P. J. Winzer, A. R. Chraplyvy, A. H. Gnauck, L. W. Stulz, R. Pafchek, and E. Burrows, J. Lightwave Technol. **22**, 249 (2004).
6. B. Moslehi, J. W. Goodman, M. Tur, and H. J. Shaw, Proc. IEEE **72**, 909 (1984).
7. L. Luo, S. Ibrahim, C. B. Poitras, S. S. Djordjevic, H. L. Lira, L. Zhou, J. Cardenas, B. Guan, A. Nitkowski, Z. Ding, S. J. Yoo, and M. Lipson, in *Conference on Lasers and Electro-Optics* (2010), paper CFL5.
8. E. J. Norberg, R. S. Guzzon, J. S. Parker, L. A. Johansson, and L. A. Coldren, J. Lightwave Technol. **29**, 1611 (2011).
9. P. Dong, N. Feng, D. Feng, W. Qian, H. Liang, D. C. Lee, B. J. Luff, M. Asghari, A. Agarwal, T. Banwell, R. Menendez, P. Toliver, and T. K. Woodward, in *Conference on Lasers and Electro-Optics* (2010), paper CThAA6.
10. S. Khaleghi, M. R. Chitgarha, O. F. Yilmaz, A. E. Willner, and M. W. Haney, in *Conference on Lasers and Electro-Optics* (2011), paper CTuW4.
11. J. Sharping, Y. Okawachi, J. van Howe, C. Xu, Y. Wang, A. Willner, and A. Gaeta, Opt. Express **13**, 7872 (2005).
12. C. Langrock, S. Kumar, J. E. McGeehan, A. E. Willner, and M. M. Fejer, J. Lightwave Technol. **24**, 2579 (2006).